TELKOMNIKA Telecommunication, Computing, Electronics and Control
Vol. 19, No. 3, June 2021, pp. 963~967
ISSN: 1693-6930, accredited First Grade by Kemenristekdikti, Decree No: 21/E/KPT/2018
DOI: 10.12928/TELKOMNIKA.v19i3.16714

Investigation on the application of ZnO nanostructures to improve the optical performance of white light-emitting diodes

My Hanh Nguyen Thi[1], Phung Ton That[2], Hoang Van Ngoc[3]
[1]Faculty of Mechanical Engineering, Industrial University of Ho Chi Minh City, Vietnam
[2]Faculty of Electronics Technology, Industrial University of Ho Chi Minh City, Vietnam
[3]Institute of Applied Technology, Thu Dau Mot University, Vietnam

Article Info

Article history:

Received May 17, 2020
Revised Aug 19, 2020
Accepted Sep 5, 2020

Keywords:

Color uniformity
Luminous flux
Mie-scattering theory
ZnO

ABSTRACT

Though combining blue LED chips with yellow phosphor has been the most common method in white light-emitting diode (WLED) production, the attained angular correlated color temperature (CCT) uniformity is still poor. Thus, this article proposes to add ZnO nanostructures to WLED packages to promote the color uniformity of the WLEDs. The outcomes of the research demonstrate that utilizing ZnO at different amount can affect the scattering energy and the CCT deviations in WLEDs packages in different extents. Particularly, adding the node-like (N-ZnO), sheet-like (S-ZnO), and rod-like (R-ZnO) leads to the corresponding decreases of CCT deviations from 3455.49 K to 96.30 K, 40.03 K, and 60.09 K, respectively. Meanwhile, with 0.25% N-ZnO, 0.75% S-ZnO, and 0.25% R-ZnO, WLED devices can achieve both better CCT homogeneity and lower reduction in luminous flux. The results of this article can be a valuable document for the manufacturer to use as reference in improving their WLED products.

Corresponding Author:

Hoang Van Ngoc
Institute of Applied Technology
Thu Dau Mot University
No 6, Tran Van On Street, Thu Dau Mot city, Binh Duong province, Vietnam
Email: ngochv@tdmu.edu.vn

1. INTRODUCTION

In illumination market, WLED devices which use the diodes to create white light have been proved to be the potential generation solid-state lighting source which can probably be an alternate to the conventional fluorescent and incandescent ones, as they perform impressive features including longevity, high efficiency, cost saving, and being eco-friendly [1-4]. One of the most popular methods to create WLED devices is freely dispensing the yellow phosphor yttrium aluminum garnet (YAG:Ce) onto a blue LED chip [5, 6]. Nevertheless, the angular correlated color temperature achieved from this method is in poor quality and the "yellow ring" phenomenon that is disadvantageous to the light performance of WLED also occurs [7-9]. Researchers proposed various methods as solutions to these problems, for example, conformal-phosphor structure [10], adjusting the surface phosphor layer [11], lens design [12], and optimizing the structure of a WLED package [13, 14]. Though the enhancement in CCT homogeneity of these approaches was confirmed, their production confronts many difficulties, and they are also expensive to use in mass production. Thus, figuring out a method that is simpler and cheaper in fabrication but still yields high CCT uniformity is essential to WLED manufacturers.

In the present, diffuser-loaded encapsulation is a promising method in enhancing the color quality of WLEDs because it can fulfill the requirements of cost-saving and simple fabrication. Adopting this concept, WLED packages with diffuser base that contains metal oxide diffuser materials (TiO_2, ZrO_2 and SiO_2) have been developed [15-18]. In the research of Chen's group [15], ZrO_2 grains whose particle size is 300 nm were integrated to the remote phosphor structure and resulted in the decrease of CCT deviation, from 1000 K to 420 K in the angles from −70° to 70°. TiO_2 diffusers (320 nm) on the phosphor or encapsulation layer were used by Lee and his partners [18]. They reported that the growth of TiO_2 concentration caused the CCT deviations to reduce. The effectiveness of these diffusers on WLED CCT uniformity is undeniable, but the focuses of aforementioned researches are the effects of a single diffuser material or different concentrations of corresponding particles. Analyses have not dug deeper into the impacts of different structures of these diffuser materials on the WLED performance [5, 19, 20]. Moreover, as there are not enough studies that provide thorough contents and specific guidance on this aspect, the process of identifying the appropriate nanoparticles to effectively enhance the color quality of WLED is very time-consuming.

These days, the scattering effects of ZnO nanostructures have been recognized, and this material is also beneficial to WLED production as it is a low-price material, and easy to control their morphologies and synthesize [21-24]. Moreover, it is possible to get many structures of ZnO by modification and control of the reaction conditions, for instances, time, temperature, and precursor concentration. The index of refraction of ZnO is 2.0 that is in between the 2.5 index of GaN and 1 of air, leading to the fact that WLEDs with ZnO has better gradient efficiency. Besides that, various researchers have been pointed out the benefit of doping ZnO into the GaN-based WLEDs, particularly with special nanostructures of ZnO, which is the enhancement of light extraction [25]. A hybrid ZnO nanostructure with microscopic cylinders and nanorods installed on light-emitting chip that can enhance the light-emitting ability of GaN-based LEDs was demonstrated by Yin's team [26]. The result from the GaN blue LEDs with ZnO nanoparticles implanted to planar indium tin oxide (ITO) film shows a growth in light emission [18]. The ZnO nanorods were used to tune the pattern of light projected from the GaN-LEDs. The improvement of light extraction efficiency was proved in these articles but the fact is that there are not many works on enhancing WLED optical performance with diffusers of ZnO morphologies which directly impact the homogeneity of both CCT and light intensity of WLED devices. Thus, this paper purpose is to study the influences of ZnO particles consisting of the node-like ZnO (N-ZnO), sheet-like (S-ZnO), and rod-like ZnO (R-ZnO). The scattering influences of ZnO nanoparticle are analyzed with Mie-scattering theory and the calculation tool MATLAB, which is presented in section 2. From the outcomes, the scattering power in WLEDs was shown to be benefited from the scattering properties of ZnO particles. Besides that, the enhancement of color uniformity responds accordingly to the fluctuation of ZnO concentration.

2. SCATTERING ANALYSIS

This section demonstrates the scattering coefficient $\mu_{sca}(\lambda)$, the scattering phase functions $S_1(\theta)$ and $S_2(\theta)$, the reduced scattering coefficient $\delta_{sca}(\lambda)$, and the scattering cross-section C_{sca} of ZnO particles. As mentioned above, the Mie-scattering theory [16-18] and MATLAB tool are utilized to calculate the light scattering effect when ZnO nanoparticles are added. The computation of ZnO scattering is expressed as:

$$\mu_{sca}(\lambda) = \int N(r) C_{sca}(\lambda, r) dr \tag{1}$$

$$g(\lambda) = 2\pi \int \int_{-1}^{1} p\,(\theta, \lambda, r) f(r)\, cos\,\theta\, dcos\,\theta\, d\,r, \tag{2}$$

$$\delta_{sca} = \mu_{sca}(1 - g) \tag{3}$$

$$S_1 = \sum_{n=1}^{\infty} \frac{2n+1}{n(n+1)} [a_n(x,m)\pi_n(\cos\theta) + b_n(x,m)\tau_n(\cos\theta)] \tag{4}$$

$$S_2 = \sum_{n=1}^{\infty} \frac{2n+1}{n(n+1)} [a_n(x,m)\tau_n(\cos\theta) + b_n(x,m)\pi_n(\cos\theta)] \tag{5}$$

- $N(r)$ is the number of diffusional particles (per cubic millimeter), or diffusional density distribution
- C_{sca} is the scattering cross-section (in square millimeters)
- λ is the wavelength of the incident light (in nanometers)
- r is the radius of each particle (in micrometers)
- θ is the scattering angle (degrees)
- $p(\theta,\lambda,r)$ is the phase function

- $f(r)$ is the size distribution function of ZnO in the phosphor layer
- $g(\lambda)$ is the anisotropy factor
- x is the size parameter
- m is the refractive index
- a_n and b_n are the expansion coefficients with even and odd symmetries, in turn
- $\pi_n(\cos\theta)$ and $\tau_n(\cos\theta)$ are the angular dependent functions.

Figure 1 and Figure 2 show that when ZnO concentrations are in the range of 0-0.25%, the scattering power distributions of the three ZnO morphology-doped films are almost unchanged, yet still different from that of the one not using ZnO. The reason is that at a low concentration, the quantity of ZnO particles are not sufficient enough to have effects on the light rays, so it is hard to see the difference among the impacts of their morphologies. Based on the general theory of scattering, as the scattering particle concentration is lower than a certain value, the scattering will be in connection with the particle cloud definitions, then the total scattered power per unit volume of space is in proportion to the scattering energy of the single particles. However, the scattering energy distribution becomes more uniform along with the amount of ZnO particles increasing in the structure.

According to the reflection method, the scattering power is greatly affected by the three ZnO morphologies. As can be seen, the S-ZnO exhibits the most powerful scattering effect in the ZnO concentration range of 0.75-2.5%, which is similar to the results of transmission measurements. From this, it is clear that using ZnO at high concentrations can homogenize the distribution of scattering power, yet the back-scattering effects are also much stronger as a result. The back-scattering energy is already high (around 0.5) even though the concentration of ZnO in the phosphor film is low at 0.25%. In Figure 3 and Figure 4, this phenomenon is demonstrated, and the higher level of backscattering energy indicates the light extraction.

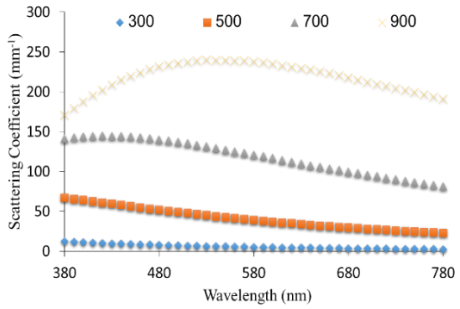

Figure 1. Scattering coefficient of ZnO particles with different diameters

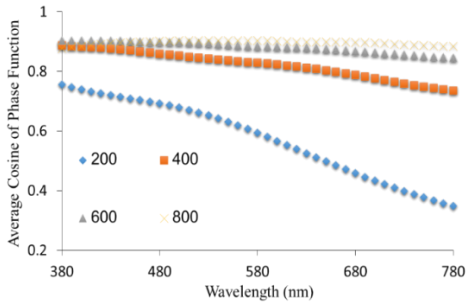

Figure 2. Phase function of ZnO particles with different diameters

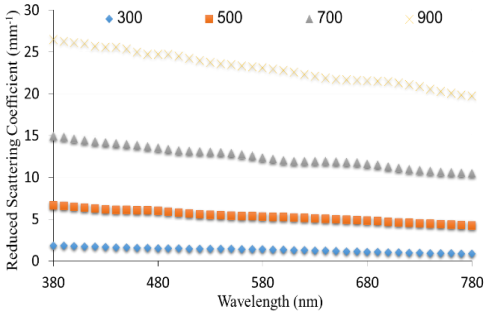

Figure 3. Reduced scattering coefficient of ZnO particles with different diameters

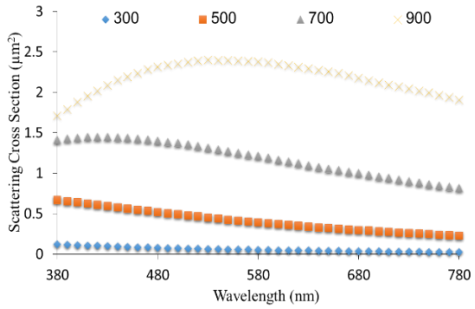

Figure 4. Scattering cross-section of ZnO particles with different diameters

3. COMPUTATION AND DISCUSSION

The LightTools 8.1.0 is the program used for the simulation of WLEDs to study the effects of ZnO-doping films on the optical properties. Each morphology of ZnO is compared and discussed to give the most thorough analysis that can help manufacturers to choose an appropriate ZnO nanostructure to enhance their WLED products. Figure 5 illustrates the diagrams of WLEDs used in this research. Each element of a WLED package is measured carefully to make sure that the experimented model is identical to the real WLED.

The specifications of LED reflector are 2.1 mm depth, 8 mm inner diameter, and 10 mm outer diameter. For the ZnO-doped phosphor film coating the nine embedded LED chips, its thickness is set at 0.08 mm.

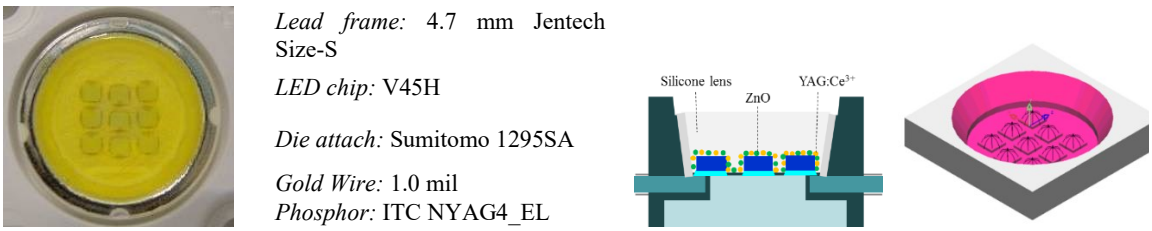

Figure 5. (a) Photograph of WLEDs sample, (b) Manufacturing parameter of WLEDs, (c) Illustration of 2D WLEDs model, and (d) the simulated WLEDs model

As discussed above, the concentrations and the morphologies of ZnO nanoparticles greatly impact the internal scattering. This section will focus on the changes of optical performances of WLEDs using ZnO as a diffuser layer. The experiments are carried out on ZnO-based WLED packages at a 350 mA driving current to investigate the scattering influences of ZnO diffuser encapsulation on the spatial distribution of CCT and light intensity, as well as the lumen efficiency. The ZnO concentration doped in the encapsulation layer is similar to that of the yellow phosphor in the traditional WLED package. Based on the results from previous analyses, it is possible to describe the angle-dependent CCT uniformity and lumious intensity as the maximum value minus the minimum one. Besides that, the spatial angles utilized to appraise the angular CCT homogeneity and luminous intensity are from −70° to 70°, as shown in Figure 6. If the light intensity is out of this range, it is weak and even cannot be used due to the "halo effect" caused by the lens or the structure of the LED packages.

Figure 7 demonstrates the luminous flux in WLEDs with various values of ZnO sizes and amounts. Though the luminous intensity of the traditional WLED package without using ZnO was relatively high (approximately 6.32 mcd), it presented poor quality. However, with ZnO-doped layers, the luminous flux can be enhanced. When N-ZnO nanoparticles are used, the WLEDs can yield higher light intensity than the other morphologies of ZnO because its transmissivity is better than the others. Meanwhile, the S-ZnO and R-ZnO-based WLEDs result in better homogeneity of light intensity, especially the S-ZnO particles, as its scattering ability is stronger than that of the other two morphologies. However, when the concentrations of ZnO increase, the luminous flux tends to decrease as the transmission becomes lower, and this phenomenon is more obvious in the case of S-ZnO nanoparticles.

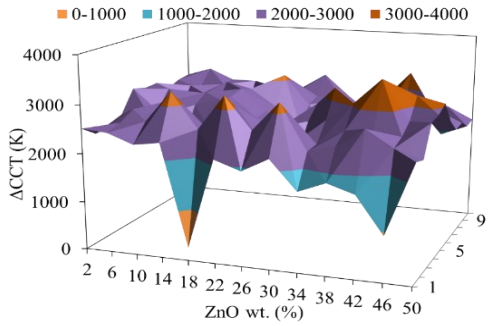

Figure 6. CCT deviations of ZnO particles with different diameters

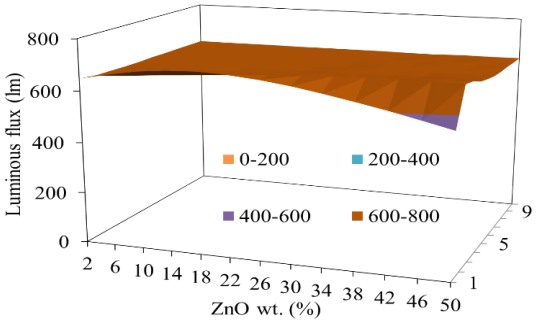

Figure 7. Luminous fluxes of ZnO particles with different diameters

4. CONCLUSION

The influences of ZnO concentrations and morphologies on the optical performances of WLEDs, including the angular CCT uniformity and lumen output, are analyzed and demonstrated. The results of the research confirm that ZnO has great effects on the WLEDs' quality due to its scattering effect. Specifically, ZnO can dramatically increase the scattering energy distribution, while the increase in its concentration results in the decline of transmission, which leads to the drop of luminous efficiency. Moreover, the decrease of luminous intensity is more considerable with the S-ZnO, compared to that of the other packages with other

ZnO morphologies. After considering the enhancement in the CCT homogeneity and the reduction of the flux, the appropriate concentrations for each morphology of ZnO nanoparticles are proposed are 0.25% for N-ZnO, 0.75% for S-ZnO, and 0.25% for R-ZnO. This article provides a detailed and practical reference for better application of ZnO in improving the light scattering effect of the diffuser layer, contributing to further developments of WLED devices.

REFERENCES

[1] X. Li *et al.*, "Projection lithography patterned high-resolution quantum dots/thiol-ene photo-polymer pixels for color down conversion," *Opt. Express,* vol. 27, no. 1, pp. 30864-30874, 2019.

[2] M. Dupont-Nivet, C. I. Westbrook, and S. Schwartz, "The role of trap symmetry in an atom-chip interferometer above the Bose-Einstein condensation threshold," *2019 Conference on Lasers and Electro-Optics Europe and European Quantum Electronics Conference*, OSA Technical Digest, Optical Society of America, 2019.

[3] S. Rasouli *et al.*, "Colorful radial Talbot carpet at the transverse plane," *Opt. Express,* vol. 27, no. 13, pp. 17435-17448, 2019.

[4] S. P. Groth *et al.*, "Circulant preconditioning in the volume integral equation method for silicon photonics," *J. Opt. Soc. Am. A,* vol. 36, no. 6, pp. 1079-1088, 2019.

[5] Z. Wen *et al.*, "Fabrication and optical properties of Pr3+-doped Ba, Sn, Zr, Mg, Ta. O3 transparent ceramic phosphor," *Opt. Lett*, vol. 43, no. 11, pp. 2438-2441, 2018.

[6] S. Lee *et al.*, "Printed cylindrical lens pair for application to the seam concealment in tiled displays," *Opt. Express,* vol. 26, no. 2, pp. 824-834, 2018.

[7] B. Swiatczak *et al.*, "Changes in fundus reflectivity during myopia development in chickens," *Biomed. Opt. Express,* vol. 10, no. 4, pp. 1822-1840, 2019.

[8] Z. Zhuang *et al.*, "Optimal ITO transparent conductive layers for InGaN-based amber/red light-emitting diodes," *Opt. Express,* vol. 28, no. 8, pp. 12311-12321, 2020.

[9] J. Ruschel *et al.*, "Current-induced degradation and lifetime prediction of 310 nm ultraviolet light-emitting diodes," *Photon. Res*, vol. 7, no. 7, pp. B36-B40, 2019.

[10] J. Li *et al.*, "Double optical gating for generating high flux isolated attosecond pulses in the soft X-ray regime," *Opt. Express,* vol. 27, no. 21, pp. 30280-30286, 2019.

[11] S. Beldi *et al.*, "High Q-factor near infrared and visible Al2O3-based parallel-plate capacitor kinetic inductance detectors," *Opt. Express,* vol. 27, no. 9, pp. 13319-13328, 2019.

[12] B. K. Tsai *et al.*, "Exposure study on UV-induced degradation of PTFE and ceramic optical diffusers," *Appl. Opt*, vol. 58, no. 5, pp. 1215-1222, 2019.

[13] S. Feng *et al.*, "Color lensless in-line holographic microscope with sunlight illumination for weakly-scattered amplitude objects," *OSA Continuum,* vol. 2, no. 1, pp. 9-16, 2019.

[14] L. He *et al.*, "Performance enhancement of AlGaN-based 365 nm ultraviolet light-emitting diodes with a band-engineering last quantum barrier," *Opt. Lett*, vol. 43, no. 3, pp. 515-518, 2018.

[15] W. Liu *et al.*, "Manipulation of LIPSS orientation on silicon surfaces using orthogonally polarized femtosecond laser double-pulse trains," *Opt. Express,* vol. 27, no. 7, pp. 9782-9793, 2019.

[16] T. R. Dastidar *et al.*, "Whole slide imaging system using deep learning-based automated focusing," *Biomed. Opt. Express,* vol. 11, no. 1, pp. 480-491, 2020.

[17] A. Udupa *et al.*, "Selective area formation of arsenic oxide-rich octahedral microcrystals during photochemical etching of n-type GaAs," *Opt. Mater. Express,* vol. 8, no. 2, pp. 289-294, 2018.

[18] J. Wang *et al.*, "Rapid 3D measurement technique for colorful objects employing RGB color light projection," *Appl. Opt*, vol. 59, no. 7, pp. 1907-1915, 2020.

[19] C. J. C. Smyth *et al.*, "27.5 W/m^2 collection efficiency solar laser using a diffuse scattering cooling liquid," *Appl. Opt*, vol. 57, no. 15, pp. 4008-4012, 2018.

[20] C. McDonnell *et al.*, "Grey-scale silicon diffractive optics for selective laser ablation of thin conductive films," *Appl. Opt*, vol. 57, no. 24, pp. 6966-6970, 2018.

[21] K. Orzechowski *et al.*, "Optical properties of cubic blue phase liquid crystal in photonic microstructures," *Opt. Express,* vol. 27, no. 10, pp. 14270-14282, 2019.

[22] R. Deeb *et al.*, "Deep spectral reflectance and illuminant estimation from self-interreflections," *Journal of the Optical Society of America A,* vol. 36, no. 1, pp. 105-114, 2019.

[23] T. Shang *et al.*, "Network selection method based on MADM and VH-based multi-user access scheme for indoor VLC hybrid networks," *Opt. Express,* vol. 26, no. 23, pp. 30795-30817, 2018.

[24] H. Jia *et al.*, "High-transmission polarization-dependent active plasmonic color filters," *Appl. Opt*, vol. 58, no. 3, pp. 704-711, 2019.

[25] X. Sun *et al.*, "Run-time reconfigurable adaptive LDPC coding for optical channels," *Opt. Express,* vol. 26, no. 22, pp. 29319-29329, 2018.

[26] D. Molter, *et al.*, "Terahertz cross-correlation spectroscopy driven by incoherent light from a superluminescent diode," *Opt. Express*, vol. 27, no. 9, pp. 12659-12665, 2019.